JOURNAL OF MATERIALS SCIENCE **36** (2001) 663–668

Triclinic oxy-hydroxyapatite

P. ALBERIUS-HENNING, E. ADOLFSSON, J. GRINS
Inorganic Chemistry, Arrhenius Laboratory, Stockholm University, SE - 106 91 Stockholm, Sweden
E-mail: peter.inorg.su.se

A. FITCH
ESRF, BP 220, F - 380 43 Grenoble Cedex, France

Partially dehydrated hydroxyapatite was characterised by X-ray powder diffraction (XRPD) using Guinier-Hägg films, diffractometer and high-resolution synchrotron data as a function of the degree of dehydration (DD). It is for the first time shown that the space group symmetry for partially dehydrated hydroxyapatite changes from hexagonal $P6_3/m$ to triclinic when more than ca. 35% of the structurally bound water is removed. With increasing DD the *a*- and *b*-axes decrease and the *c*-axis increases. At the highest DD value attained (78%) before the onset of a decomposition of the apatite, the cell parameters were determined to be $a = 9.40023\ (3)$, $b = 9.39704\ (3)$, $c = 6.89967\ (2)$ Å, $\alpha = 90.0626\ (2)^\circ$, $\beta = 89.7478\ (1)^\circ$ and $\gamma = 119.9971\ (2)^\circ$. A structure refinement for this sample converged with $R_F = 3.7\%$ in space group $P\bar{1}$, using synchrotron data ($\lambda = 0.852790$ Å), 795 reflections in the 2θ range 5–45° and 62 positional parameters. The shifts of the atoms from their corresponding positions in hexagonal hydroxyapatite are small. A possible cause for the triclinic distortion is a tilting of the hydroxide ions in the apatite channels away from the channel axis.

1. Introduction

The high-temperature characteristics of hydroxyapatite, $Ca_5(PO_4)_3OH$, (OHAp) has been a matter of debate since 1933, when dehydrated hydroxyapatite, (O, OH)Ap, was first reported [1]. The subject has received a lot of attention since then due to the importance of hydroxyapatite, being the main inorganic constituent of all vertebrates. In man, impure OHAp constitutes 55% (by weight) of the skeleton and 96% of the enamel [2]. Since the beginning of the seventies [2–4] sintered hydroxyapatite has been used as an implant material, which has further increased the number of studies.

The existence of completely dehydrated OHAp, oxyapatite, has been the subject of controversy [5] but it's existence seems now to be commonly accepted [6, 7]. The behaviour of partially dehydrated hydroxy apatite is however still not well understood and there are a lot of contradictory results in the literature. The lack of consistency is mainly due to the poor (if any at all) methods used for a quantitative determination of the residual water content of the dehydrated samples. The present study was motivated by a need for a proper characterisation of apatite samples prepared at high temperature and intended for e.g. implants, since the physical properties are highly dependant on the quality of the apatite [8].

The hexagonal hydroxyapatite structure contains two hydroxide ions per unit cell, positioned on the hexad close to the calcium triangles positioned at $z = 0.25$ and $z = 0.75$ [9]. Hydroxyapatite dehydrates on heating according to the following reaction [6]:

$$Ca_5(PO_4)_3OH \rightarrow Ca_5(PO_4)_3(OH)_{1-X}O_{X/2} + X/2H_2O \quad (1)$$

The dehydration of stoichiometric OHAp starts at approximately 600°C [10] and increases with increasing temperature, finally the apatite collapses into tricalcium phospate, $Ca_3(PO_4)_2$, and tetracalcium phosphate, $Ca_4(PO_4)_2O$ according to [11]:

$$2Ca_5(PO_4)_3(OH)_{1-X}O_{X/2} \rightarrow 2Ca_3(PO_4)_2 + Ca_4(PO_4)_2O + (1-X)H_2O \quad (2)$$

The kinetics of the rehydration of (O, OH)-Ap are retarded by lowering the temperature. At room temperature, dehydrated samples are stable, and even so if they are heated up to 115°C in water vapour [12, 13]. A study of the physical properties of (O, OH)Ap, such as cell parameters, is thus possible at room temperature.

There are several studies that describe the dehydration of hydroxyapatite as a function of temperature and water pressure [14–16] and many that describe the cell parameters as a function of dehydration [12, 13, 17–19]. However, in none of these is the evaluation of the cell parameters at room temperature determined in parallel with an experimental quantification of the degree of dehydration (DD). In [6] the cell parameters of oxyapatite (OAp) were determined but this was done at elevated temperatures in order to prevent rehydration.

In the present study, hydroxyapatite has been dehydrated to different DD ranging from 0 up to 84%. The water content has been quantitatively measured and the unit cell parameters accurately determined. As the apatite is dehydrated the *a* and *b* axes are found to decrease and the *c*-axis to increase. For the first time it is shown that partially dehydrated apatite undergoes a phase transition from hexagonal to triclinic, a fact that may be very useful for the characterisation of heat-treated apatitic samples. The crystal structure of a sample with a DD of 78% has also been refined using the Rietveld method and synchrotron powder X-ray diffraction data to $R_F = 3.7\%$.

2. Experimental

Hydroxyapatite, Merck, was dehydrated at different temperatures under vacuum in a tube furnace. All samples were preheated in air at 1200°C for two hours in order to increase the grain size of the precipitated OHAp, and thus decrease the amount of surface adsorbed water. The samples were then put in an evacuated quartz tube and heated at a rate of 400°C/h up to the dehydration temperature. Reaching the dehydration temperature (750–1250°C) the quartz tube was flushed with argon (99.999%) and then evacuated. The argon flushing was repeated every 20 minutes for two hours. The argon flushing, followed by evacuation to a total pressure of 1Pa, was found important in order to reduce the partial water pressure to a minimum since water is evolved during dehydration (Equation 1). After a final argon flushing, the quartz tube was sealed and the temperature decreased to 25°C at 400°C/h.

The water content of the dehydrated samples was quantitatively determined using a high temperature gravimetric analyzer (Setaram TAG24) by heating the samples from room temperature to 1500°C under argon (99.999%). Hydroxyapatite is completely dehydrated at 1450°C whereupon the structure collapses [12, 15] and the procedure thus gives an absolute quantification of the water content in the partially dehydrated apatites.

Three different XRPD techniques were used to characterise the dehydrated samples: Guinier-Hägg films, powder diffractometry and high-resolution powder diffractometry at a synchrotron source. The Guinier-Hägg films were recorded using Cu-K_{α_1} radiation and Si as internal standard, and evaluated using a scanner system [20]. Powder diffraction patterns were also recorded, for all dehydrated samples studied, with a STOE STADI/P diffractometer, Cu-K_{α_1} radiation, the samples mounted in capillaries with 1 mm diameter and a small linear position sensitive detector, covering 4.6° in 2θ, that was moved in steps of 0.2°. XRPD data for two dehydrated samples (DD = 39 and 78%) were collected on the beam line BM16 at the ESRF, Grenoble, in the 2θ range 1–57°, with $\lambda = 0.852790$ Å and the samples contained in 1 mm diameter spinning capillaries. The detector arm, with its nine detectors, was scanned at a contineous rate of 0.5 degrees min^{-1}, and the electronic scalers and 2θ encoder were read every 200 ms. The data were subsequently normalised, and rebinned, and the counts from the nine channels combined, to yield the equivalent scan with a step of 0.002°. Structure refinements using the Rietveld method were carried out with the program packages GSAS [21] and Fullprof [22].

3. Results

This study comprises an investigation of the detailed structural changes of hydroxyapatite occurring as it dehydrates thermally to oxy-hydroxy apatite as a function of different DD. Ten samples of hydroxyapatite were dehydrated at various temperatures between 750°C and 1200°C yielding samples with DD ranging from 3% up to 84%. The obtained samples were characterised using thermogravimetric analysis (TGA) and XRPD.

3.1. TGA

When hydroxyapatite dehydrates, a maximum of one water molecule per unit cell can be removed according to Equation 1. Upon complete dehydration of OHAp the weight loss is 1.79%. It is thus possible to quantify the degree of dehydration by measuring the amount of residual water that is left in the structure after the dehydration using TGA. The DD is defined as:

$$\mathrm{DD} = \frac{1.79 - \mathrm{WD}}{1.79} \times 100 \qquad (3)$$

where WD stands for the weight decrease in percent upon heating to 1500°C. Results from two typical TGA experiments are given in Fig. 1. The WD is thus determined from the weight difference between levels *a* and *b*. The increase in weight shown by the lower curve, starting at 600°C, is due to *in situ* rehydration of the dehydrated sample [11] and does not affect the final results since the sample becomes completely dehydrated at 1450°C. The results from the whole series of dehydration experiments are shown in Fig. 2 where they are compared to findings from [14].

3.2. XRPD

For the dehydrated samples a splitting of reflections was observed in Guinier-Hägg and diffractometer XRPD patterns that increased with the DD, indicating a lower space group symmetry for these than the hexagonal

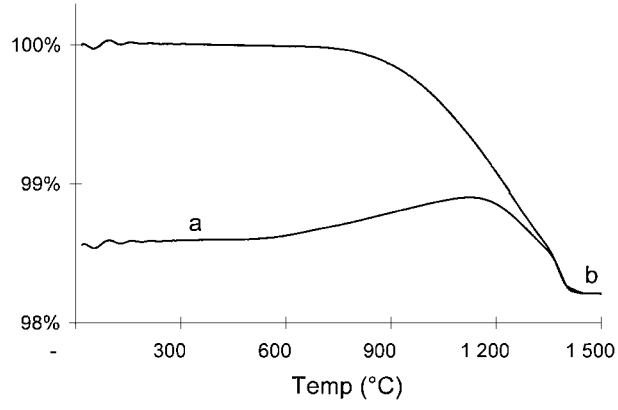

Figure 1 Typical TGA runs for determining the DD for partially dehydrated hydroxyapatite. The lower curve is for a sample dehydrated at 1150°C and the upper one for a non-dehydrated sample. The lower curve was moved so that the two curves meet at b.

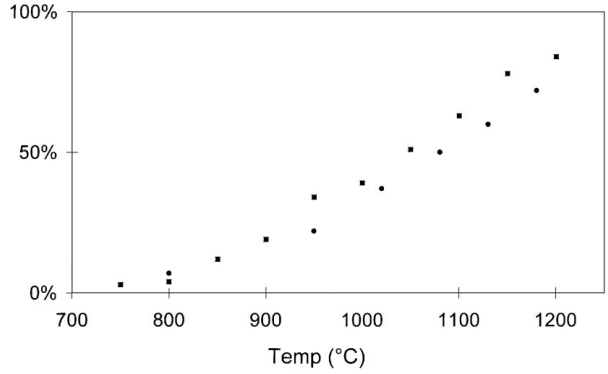

Figure 2 The DD as a function of dehydration temperature (squares). The results from [14] are shown for comparison (circles). The DD is systematically higher for the data from the present study, indicating a lower water vapour pressure at the dehydration temperature.

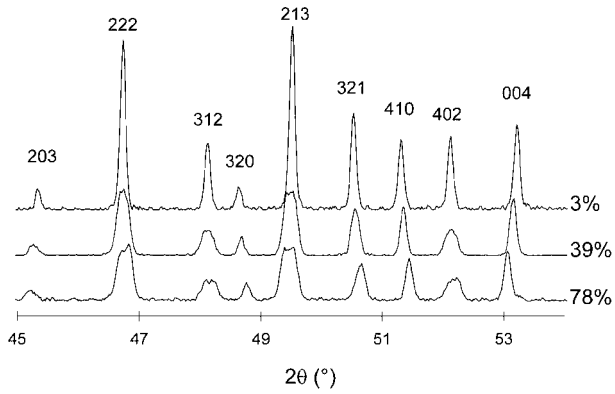

Figure 3 Diffractometer XRPD patterns for a series of samples with different DD, illustrating the progressive triclinic distortion and shifts in units cell parameters.

$P6_3/m$ symmetry for hydroxyapatite ($P2_1/b$ when perfectly stoichiometric and ordered [23]). Diffractometer powder patterns in the 2θ range 45–55° (Cu-K_{α_1}-radiation) are shown in Fig. 3 for a series of dehydrated samples, illustrating the corresponding increase in the splitting of reflections as well as shifts in reflection positions. The splitting was initially attributed to a monoclinic distortion of the hexagonal cell but the synchrotron XRPD (Fig. 4) data with their superior resolution clearly showed the distortion to be triclinic. Reflections *h*00, 0*k*0 and 00*l* were furthermore found to be sharp and symmetrical, indicating that the samples were mono-phasic and homogeneous. Unit cell parameters obtained from synchrotron data for the two samples with DD = 39 and 78% are given in Table I and compared to unit cell parameters from stoichiometric

TABLE I Cell parameters of hydroxyapatite [23] compared to dehydrated oxy-hydroxyapatite. Unit cell parameters are shown in Ångström (Å) units and the angles in degrees (°)

	DD = 0%	DD = 39%	DD = 78%
a	9.4214 (8)	9.41009 (3)	9.40023 (3)
b	9.4214 (8)	9.41258 (3)	9.39704 (3)
c	6.8814 (7)	6.88301 (1)	6.89967 (2)
α	90	90.0371 (2)	90.0626 (2)
β	90	89.8506 (1)	89.7478 (1)
γ	120	120.0014 (1)	119.9971 (2)
V	528.98	527.963 (2)	527.833 (9)

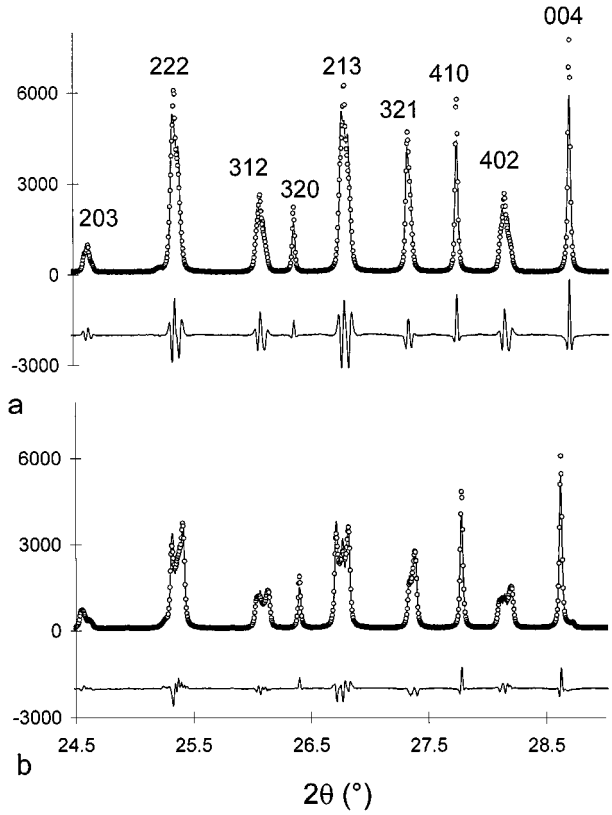

Figure 4 Observed (circles), calculated (line) and difference (bottom) synchrotron XRPD patterns for hydroxyapatite dehydrated at (a) 1000°C and with DD = 39% and (b) at 1150°C and with DD = 78%.

OHAp [23]. The distortion of the hexagonal unit cell is found to be connected mainly with a deviation from 90° for the angles α and β, while the γ angle is very close to 120° and the *a* and *b* axes of very similar length. The distortion can accordingly be essentially regarded as a small tilting of the *c* axis.

Refined values of unit cell axes for samples with other DD were determined using Guinier-Hägg data, with the 2θ scale corrected by the use of Si as internal standard. The unit cell angles α and β could however not be reliably obtained from these data which therefore were fixed at values obtained from corresponding refinements using diffractometer data. Furthermore, two approximations were made: the γ angle was set to 120° and the *a* and *b* axes set to equal length. The esd's were on the average 0.0004° and 0.0002° for the angles α and β, respectively, and 0.0003 Å for the cell axes. For the sample dehydrated at 950°C the triclinic distortion was found to be very small and the esd's in the angles α and β larger by a factor of 4.

A rough comparison of the three diffraction techniques used may be made with respect to resolution and number of reflections covered. The 2θ ranges used were 9.1–89.5° (ca. 850 reflections), 10–90° (ca. 860 reflections), 5–45° (945 reflections) for the film, diffractometer and synchrotron data, respectively, and the respective half-width for the $1\bar{3}3$ reflection 0.095° ($2\theta = 49.4°$), 0.082° ($2\theta = 49.4°$) and 0.027° ($2\theta = 26.8°$). The reflection intensities were furthermore more reliable for the diffractometer data than the film data and superior for the synchrotron data.

The variation of the cell parameters as a function of the degree of dehydration is shown in Fig. 5. The *a*

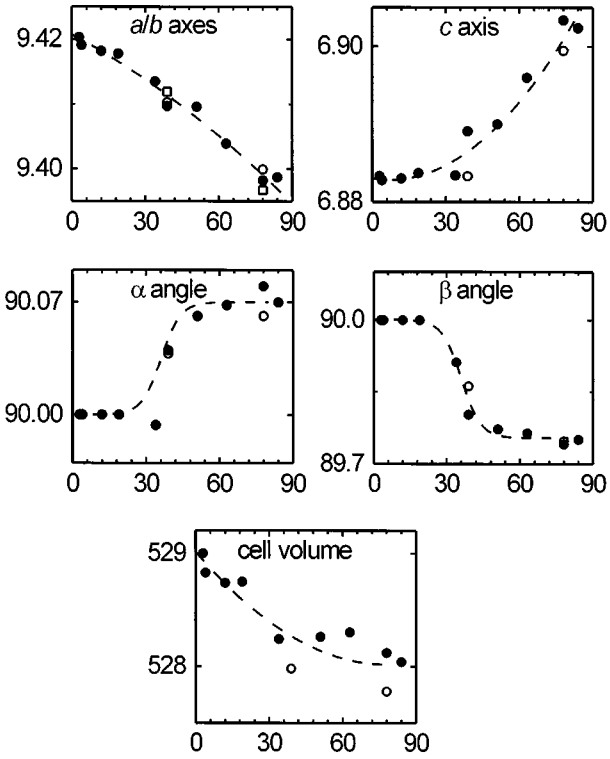

Figure 5 Unit cell parameters (Å), angles (°) and volumes (Å^3) for partially dehydrated hydroxyapatite versus the DD. Filled circles are results from GH and diffractometer data, open circles and squares are results from synchrotron data.

(and *b*) axis shows a nearly linear decrease with the DD while the *c* axis is constant up to a DD of approximately 35%, the value at which the triclinic distortion could first be discerned, and increases then linearly with increasing DD. The α and β angles appear to increase and decrease, respectively, rapidly around DD = 35% (within an approximately 10% wide DD range) and are comparatively constant for DD values above ca. 45%. The unit cell volume decreases in a linear way up to ca. DD = 35% and is relatively constant at higher DD values.

3.3. Rietveld refinements using synchrotron data

The crystal structure of the sample dehydrated at 1150°C was refined by the Rietveld method and using the synchrotron data set collected at ESRF. The two refinement programs used, GSAS and FullProf, yielded essentially the same results and only results from the latter will be described. Of the two possible triclinic space groups, $P\bar{1}$ was chosen since the hydroxide and oxide ions can be assumed to be disordered around the initially present mirror planes at $z = 1/4$ and $z = 3/4$. Starting values for atomic positional parameters were taken from [9] and a Debye-Scherrer type absorption correction applied with $\mu R = 1.4$ (corresponding to a sample packing density of 60%). After refining profile function (Thompson-Cox-Hastings pseudo-Voigt) parameters, background, unit cell parameters and a common temperature factor, the R_F factor was 8.1% for 795 reflections in the 2θ range 5–45°. Isotropic temperature parameters were then refined, keeping them equal for structurally equivalent atoms (*vis-à-vis* the hydroxy

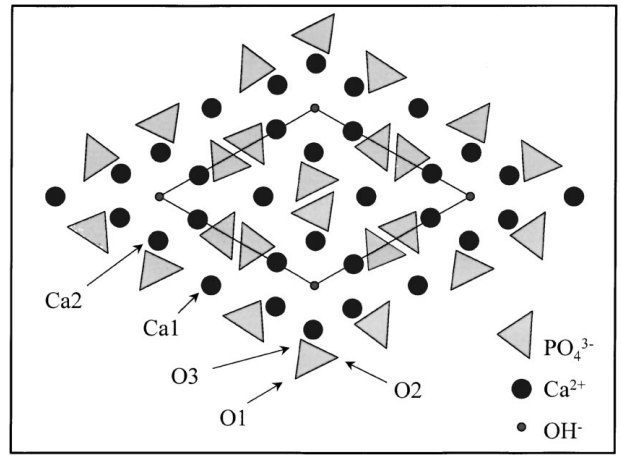

Figure 6 Illustration of structure of hexagonal hydroxyapatite projected along [001]. The crystallographically different oxygen- and calcium atoms are indicated.

apatite) in parallel with the site occupancy factor for the hydroxide-oxygen (all other atom sites assumed to be fully occupied) resulting in a decrease of R_F to 7.4%. It is notable here that the refined values for the thermal displacement factors were larger for atoms closer to the *c*-axis and the disordered hydroxide-oxide position. The temperature parameters for the O3*i* atoms, with *i* denoting the set of atoms corresponding to symmetry related atoms in hexagonal hydroxyapatite, (see Fig. 6) were four times larger than those for O1*i* and the temperature parameters for Ca2*i* were 30% larger than for Ca1*i*. In the final refinement 62 atomic positions were refined with (i) the isotropic temperature parameters restricted to be equal for groups of atoms originating from the same atom in hexagonal OHAp, (ii) the displacement of the two oxygen atoms, O4*a* and O4*b*, from the pseudo-mirror planes at $z = 1/4$ and $z = 3/4$ kept equal, (iii) the occupancy of the O4*a* and O4*b* were kept equal and (iv) all other atom sites were assumed to be fully occupied. The refinement converged with $R_F = 3.7\%$, $R_p = 7.0\%$, $R_{wp} = 9.2\%$ Dwd = 0.34 and $\chi^2 = 13.7$. A corresponding refinement for the sample dehydrated at 1000°C and with DD = 39% yielded somewhat larger residual factors. The fit between observed and calculated powder patterns are shown in Fig. 6 for the 2θ range 24–29°. The progressive splitting of hexagonal reflections with increasing DD is clearly visualised. The high χ^2 value for the sample with DD = 78% implies however that the observed pattern is not modelled entirely correct. An inspection shows that in the observed pattern the reflections of the type (00*l*) and (*hk*0) are sharp while groups of overlapped (*hkl*) reflections appear to have smoother observed profiles than calculated ones. In the refinement programs used a preferential broadening is modelled by functions that increase or decrease with the angle relative a chosen crystallographic direction. These functions appear to be inadequate for the present case and we have not been able to amend the profile fit.

Although the R_F value decreased by a factor of 2 when the positional parameters were refined, the shifts of the atoms from their initial hexagonal positions were on the whole small and in many cases insignificant. Increasing the end limit of the 2θ range in a refinement

TABLE II Structural parameters for hydroxyapatite dehydrated at 1150°C and with DD = 78% from XRPD synchrotron data. Numbers in brackets are standard deviations. The calculated differences Δ in Å relative the positions in hexagonal hydroxyapatite [9] are also given. The refined site occupancy factor for the O4 atoms is 0.37(1)

Atom	x	y	z	β(Å^2)	Δ(Å)
Ca1*a*	0.3372 (18)	0.6630 (24)	0.0018 (18)	1.0 (1)	0.06 (2)
Ca1*b*	0.6693 (21)	0.3300 (24)	0.5039 (18)	1.0	0.05 (2)
Ca2*a*	0.2402 (21)	0.9929 (18)	0.2441 (18)	1.6 (1)	0.07 (2)
Ca2*b*	0.0102 (21)	0.2543 (18)	0.2577 (21)	1.6	0.06 (2)
Ca2*c*	0.7411 (21)	0.7496 (18)	0.2495 (18)	1.6	0.05 (2)
Pa	0.3987 (27)	0.3692 (24)	0.2543 (24)	1.0 (1)	0.03 (2)
Pb	0.6309 (27)	0.0248 (21)	0.2510 (24)	1	0.05 (2)
Pc	0.9723 (24)	0.6070 (24)	0.2433 (27)	1	0.07 (2)
O1*a*	0.327 (6)	0.477 (5)	0.267 (5)	0.8 (3)	0.13 (3)
O1*b*	0.511 (5)	0.840 (5)	0.253 (5)	0.8	0.05 (3)
O1*c*	0.160 (5)	0.676 (5)	0.234 (5)	0.8	0.11 (3)
O2*a*	0.585 (5)	0.461 (5)	0.272 (5)	1.5 (3)	0.16 (3)
O2*b*	0.535 (5)	0.120 (5)	0.223 (5)	1.5	0.19 (3)
O2*c*	0.881 (6)	0.424 (5)	0.256 (5)	1.5	0.12 (3)
O3*a*	0.345 (6)	0.259 (6)	0.063 (5)	2.3 (3)	0.07 (3)
O3*b*	0.773 (5)	0.066 (5)	0.101 (5)	2.3	0.47 (3)
O3*c*	0.905 (6)	0.641 (5)	0.059 (5)	2.3	0.15 (3)
O3*d*	0.660 (5)	0.745 (6)	0.572 (5)	2.3	0.05 (3)
O3*e*	0.270 (6)	0.903 (6)	0.558 (5)	2.3	0.21 (4)
O3 *f*	0.074 (6)	0.328 (6)	0.586 (5)	2.3	0.17 (4)
O4*a*	0.000 (15)	0.979 (19)	0.212 (9)	3 (2)	0.24 (10)
O4*b*	0.990 (15)	0.986 (20)	0.712 (9)	3 (2)	0.18 (10)

to 57° did not improve the determination of atomic positions. Refinements using anisotropic temperatures factors did furthermore not indicate any substantial anisotropy, with the exception of O4 atoms for which the displacements were larger along the *c*-axis, or result in a better fit. The final atomic positions are given in Table II with the the esd's from the refinement multiplied by a factor of 3 to account for serial correlation [24]. The refined value of the site occupancy factor for the O4*a*, *b* atoms was 0.37(1), giving an average of 1.48 oxygen atoms per unit cell. This agrees quite well with the TG data giving a DD of 78% which corresponds to an average of 1.22 oxygen atoms per unit cell. Computed shifts Δ in Å for atomic positions relative to those for hexagonal OHAp are also given in Table II, calculated by using hexagonal coordinates from [9] and the triclinc cell. For the metal atoms the Δ values are on the average 0.06 Å, corresponding to ca. 3 esd's, and for the oxygen atoms, excluding the O3*b* atom, on the average 0.14 Å, corresponding to roughly 4.5 esd's. The shifts (Δ) observed for the O3*b* atom is larger than for the other oxygen atoms, 0.47(3) Å. We do not have any explanation for this since we do not see any reason to structurally distinguish the O3*i* atoms.

The comparatively large temperature factors for the O4*a* and O4*b* atoms is expected in view of that this site is occupied by either an oxide- or a hydroxide oxygen atom. A structure determination of an oxide-ion containing calcium apatite, $Ca_{15}(PO_4)_9IO$ [25], has shown that the oxide-ion is positioned closer to the mirror plane at $z = 1/4$ than is the hydroxide ion. Attempts to refine the O4*a* and O4*b* as split positions were not successful. A larger static disorder, as indicated by larger thermal displacement parameters, of the atoms facing the hexad (Ca2- and O3 atoms) may likewise be caused by the statistical occupancy of hydroxide and oxide ions. The Ca2*i* atoms have three different surroundings depending on whether the centre of the Ca2*i*- triangle is occupied by a hydroxide ion, an oxide ion or if it is vacant. The triangle of Ca2*i* atoms will behave differently in these three situations, it will expand around a vacancy and contract around an oxide ion as compared to when the Ca2*i* triangle is filled with a hydroxide ion [7, 23]. For the oxygen's facing the hexad (O3*i*) the situation is more complex since e.g. the O3*i*-triangle close to $z = 0.1$ will have at least five different surroundings, four cases corresponding to hydroxide or oxide ions positioned at $z = 0.2$ or $z = 0.8$, respectively, and a fifth case to when both the positions at $z = 0.2$ and $z = 0.8$ positions are vacant. One reason for a larger static disorder for O2*i* than O1*i* atoms may be the close contact (2.408(9) Å [9]) between O2*i* and the disordered Ca2*i*, with displacements of the latter possibly influencing the position of the former.

The available data do not allow us to make any definitive conclusions concerning the origin of the triclinic distortion. It is however most probably connected with the hydroxide ion which in hydroxyapatite is aligned along the *c*-axis and with the hydrogen atom pointing away from the Ca2*i* triangle [9]. If there is a vacancy adjacent to the hydroxide ion (in the direction of the hydrogen) the hydroxide ion is completely free to tilt in any arbitrary direction. The O4-H-O3 distance in OHAp is 3.07 Å which is long for a hydrogen bond, but if an O4*i* atom is allowed to move towards one of the O3*i* atoms, a hydrogen bond may form. The possibility of tilting hydroxide ions is supported by an investigation of γ-ray irradiated OHAp in which tilted hydroxide ions neighbouring vacant hydroxide positions was reported [26], although no triclinic cell distortion was observed in that case. Considering however that the vacancy concentration is higher for the dehydrated apatites it seems possible that a hydroxide-tilting may cause the small tilting of the c-axis observed in our study.

4. Concluding remarks

For the first time it is shown that partially dehydrated hydroxyapatite is triclinic. The hexagonal-triclinic phase transformation occurs at ca. 35% DD. The variation of triclinic unit cell parameters with the DD may be very useful for an estimation of the quality of synthetic hydroxyapatite samples produced via high-temperature methods.

References

1. M. A. BREDIG, H. H. FRANCK and H. FÜLDNER, *Z. Elektrochem.* **39** (1933) 959.
2. H. AOKI, "Science and Medical Applications of Hydroxyapatite" (Takayama Press System Center Co., Inc, Tokyo, 1991).
3. S. R. LEVITT, P. H. CRAYTON, E. A. MONROE and R. A. CONDRATE, *J. Biomed. Mater. Res.* **3** (1969) 683.
4. E. A. MONROE, W. VOTAVA, D. B. BASS and J. MCMULLEN, *J. Dent. Res.* **50** (1971) 860.
5. D. MCCONNELL and M. H. HEY, *Mineral. Mag.* **37** (1969) 301.
6. J. C. TROMBE and G. MONTEL, *J. Inorg. Nucl. Chem.* **40** (1978) 15.

7. P. ALBERIUS HENNING, A. R. LANDA-CÁNOVAS, A.-K. LARSSON and S. LIDIN, *Acta Cryst.* **B55** (1999) 170.
8. P. DUCHEYNE, S. RADIN and L. KING, *J. Biomed. Mater. Res.* **27** (1993) 25.
9. M. I. KAY, R. A. YOUNG and A. S. POSNER, *Nature* **204** (1964) 1050.
10. E. ADOLFSSON, MATS NYGREN and L. HERMANSSON, *J. Amer. Ceram. Soc.* **82** (1999) 2909.
11. E. ADOLFSSON, Thesis, Kista Snabbtryck AB, Stockholm, 1999.
12. J. ZHOU, X. ZHANG, J. CHEN, S. ZENG and K. DE GROOT, *J. Mater. Sci. Mater. Med.* **4** (1993) 83.
13. R. M. H. VERBEECK, H. J. M. HEILIGERS, F. C. M. DRIESSENS and H. G. SCHAEKEN, *Z. Anorg. Allg. Chem.* **466** (1980) 76.
14. A. M. J. H. SEUTER, *React. Solids*, Proc. Int. Symp., 7th (1972) 806.
15. B. LOCARDI, U. E. PAZZAGLIA, C. GABBI and B. PROFILO, *Biomaterials* **14** (1993) 437.
16. A. J. RUYS, M. WEI, C. C. SORRELL, M. R. DICKSON, A. BRANDWOOD and B. K. MILTHORPE, *ibid.* **16** (1995) 409.
17. T. KIJIMA and M. TSUTSUMI, *J. Amer. Ceram. Soc.* **62** (1979) 455.
18. K. A. GROSS, C. C. BERNDT, P. STEPHENS and R. DINNEBIER, *J. Mater. Sci.* **33** (1998) 3985.
19. J. C. TROMBE, *Ann. Chim. (Paris)* **8** (1973) 335.
20. K. E. JOHANSSON, T. PALM and P.-E. WERNER, *J. Phys. E* **13** (1980) 1289.
21. A. C. LARSON and R. B. VON DREELE, Los Alamos Nat. Lab. Rep. No LA-UR-86-748, 1987.
22. J. RODRIGUEZ-CARJAVAL, Laboratoire Léon Brillouin (CEA-CNRS), 1997.
23. J. C. ELLIOTT, P. E. MACKIE and R. A. YOUNG, *Science* **180** (1973) 1055.
24. J.-F. BERÁR and P. LELANN, *J. Appl. Crystallogr* **24** (1991) 1.
25. P. ALBERIUS HENNING, S. LIDIN and V. PETRÍCEK, *Acta Cryst.* **B55** (1999) 165.
26. M. MENGEOT, R. H. BARTRAM and O. R. GILLIAM, *Phys. Rev. B* **11** (1975) 4110.

Received 14 September 1999
and accepted 27 June 2000